Investigation on the temperature compensating model for ring laser gyroscope

Chuang Guo (郭 创)[1], Yongjun Xu (胥勇军)[1], and Xiaoning Zhao (赵小宁)[2]

[1]*Engineering Institute, The Air Force University of Engineering, Xi'an 710038*
[2]*Flight Automatic Control Research Institute, Xi'an 710065*

Received February 27, 2006

Thermal effects impose the greatest limit on the precision of a ring laser gyro (RLG). Selections of temperature sensing points were comparatively discussed based on large numbers of experimental data to improve its precision, and the optimum combination was selected to establish a practical compensating model. The model is applied to new experimental data under the given and varied temperatures. Results show that the bias trend changing with the temperature is basically eliminated and the bias stability is enhanced significantly.

OCIS codes: 140.3370, 060.2800, 120.6810, 120.6780, 070.6020.

Ring laser gyroscope (RLG) is a kind of optical gyroscope by means of the Sagnac effect, and it is one of the most ideal devices for the Strapdown Inertial Navigation System (SINS). But the temperature characteristic of RLG brings lots of inverse influence and confines the further increase of its precision. Therefore, necessary temperature control or temperature compensating measures must be put into practice in order to improve gyroscope precision when it is requested to work in high accuracy situation. Generally, we always adopt the soft technique such as temperature compensating.

The temperature field becomes complex when the RLG is working, the compensating model is difficult to realize high-precision, many scholars have made in-depth study, their works[2−5] mostly concentrate on the mechanism analysis of RLG and test data processing. Little work is done in the selection of the sensor position. With those model to compensate some RLG, the compensating effect is not well. In the course of building the right model, selection of the sensor position (temperature sensing point) is an important factor.

On the basis of lots of environmental temperature experiments, we analyze the choice of several temperature sensing points of some RLG, and select the best temperature sensing point to set up model, at the same time, the model is validated experimentally.

A typical quadrangular high-precision single-axis RLG is shown in Fig. 1. There is a quadrangular beam of light channel in the cavity, and the reflectors are installed in four big holes at the top angles. There are two anodic subassemblies and a public cathode in the RLG.

Fig. 1. High-precision single-axis RLG.

This structure has some more typical applications than other ones, internationally which mainly include LG8028 and LG9028 (American company Litton), GLS16 and GlS32 (French company SAGEM), and SINGLE33 and Pixyz22 (French company SEXTENT), etc..

Temperature is the main cause to the change of bias, as depicted in Refs. [1—4], which is the primary error source to the RLG, the temperature influences on the RLG mainly behave in the following several aspects.

Firstly, in view of the hot source, when RLG is working, it will have a fever, the course to achieve balance will always spend several hours, furthermore, the temperature field of RLG will become very complex when the surrounding temperature is changing, and it is difficult to keep balance.

Secondly, in view of the physics characteristic, gaseous refractive index, heat transmits coefficient of material, and optical characteristic of optical devices etc will change with the variety of temperature.

Thirdly, in view of the geometrical characteristic, thermal expansion, shrink, and flexural deformation will all lead to the change of optical loop. It will result in the increase of the resonance system's spoilage.

When the resonant cavity length changes with the temperature, the relative error can be expressed as

$$\eta = \frac{\Delta L}{L} = \frac{\Delta T \cdot L \cdot \alpha}{L} = \alpha \cdot \Delta T, \tag{1}$$

where L is the resonant cavity length, ΔL variance of length, ΔT variance of temperature, and α thermal expansion coefficient.

At present time, Zerodur crystallite glass materials mostly produced in Germany are usually used to manufacture the high-precision RLG. Its thermal expansion coefficient is 5×10^{-8} °C^{-1}, when the variance of temperature is 100 °C, the relative error is 5 ppm, from the formula of scale factor $K \approx L/4\lambda$, we can see that its effect which will cause the variety of bias cannot be ignored.

At last, the change of the temperature field will arouse the change of airflow field, which will make an imbalance of the discharging current between the two arms and make the bias influence come from Lanmiaoer-flow effect worse[3].

A certain high-precision RLG is a typical quadrangle, single shaft, mechanism dithering RLG. We install some temperature-sensors in such position as the anode, the cathode, the cabinet etc., they are denoted with P1, P2, P3, P4 respectively. The install positions are shown in Fig. 2.

According to the national military standard "Methods for laser gyroscope test" GJB2427-1995, we have a bias test of RLG in the given surrounding temperature such as +50 °C, +40 °C, +30 °C, +20 °C, +10 °C, 0 °C, −10 °C, −20 °C, −30 °C and so on, the corresponding temperature measured in the four positions is denoted with T_1, T_2, T_3, T_4.

Whether the choice of the temperature-sensor position is right or not, which will influence the temperature that can reflect the thermal change of the RLG. That is to say, it can influence the correlation between the temperature and the bias. The mutative characteristic of the bias in different temperature sensing points determines how to choose the right sensing point in the compensating model. Here we only consider the typical condition when the surrounding temperature is 0 °C to explain it.

When the temperature-sensor is pasted on the angular rate sensor (P1), temperature T_1 and the mutative curve of the bias are shown in Fig. 3. Temperature goes up 1.5 °C during the whole test, and the bias changes relatively even.

When temperature-sensor is pasted on the anode (P2), temperature T_2 and the mutative curve of the bias are shown in Fig. 4. Temperature goes up 2.5 °C during the whole test, and the bias changes relatively even firstly,

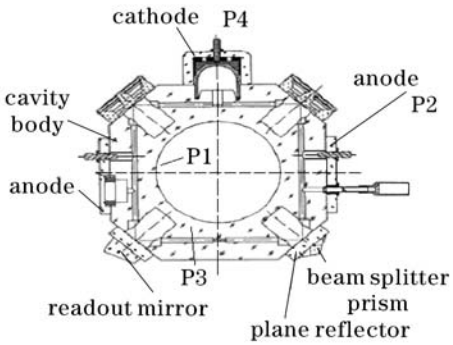

Fig. 2. Installation position of temperature sensor in a certain RLG.

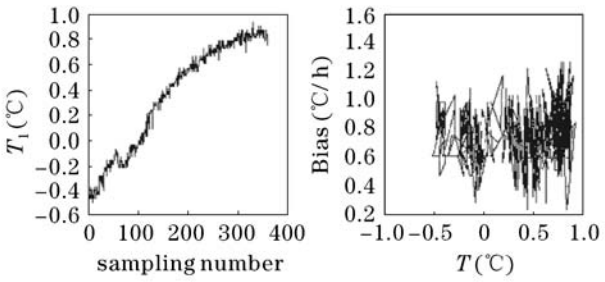

Fig. 3. Mutative curves of temperature and its bias with temperature on the position P1.

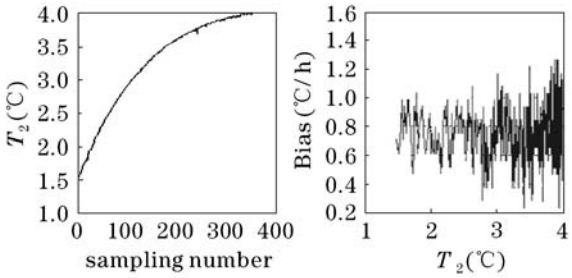

Fig. 4. Mutative curves of temperature and its bias with temperature on the position P2.

and then acutely. This is because that the foregoing temperature changes very acutely, and the posterior temperature changes tardily.

When temperature-sensor is pasted on the cabinet (P3) or pasted on the cathode (P4), the changes is different, see in Ref. [5].

The characteristic of temperature and mutative curve of the bias measured in the temperature-sensor position, which determines that we should select the best position, can reflect the performance variance of RLG as the independent variable to build the model.

Considering the RLG Inertial Navigation System is applied in the aircraft, working time is long, and the demand for precision is relatively high. During meticulous riddling, the compensating model is based on the variety and the temperature grads. The model based on the temperature sensing points T_1 and T_2 is

$$\begin{cases} B = B_0 + a_1 \times (T_1 - T_{10}) + a_2 \times (T_1 - T_{10})^2 \\ \quad +a_3 \times (T_2 - T_1) \\ \begin{cases} a_1 = A_{10} + A_{11} \times T_{10} + A_{12} \times T_{10}^2 \\ a_2 = A_{20} + A_{21} \times T_{10} + A_{22} \times T_{10}^2 \\ a_3 = A_{30} + A_{31} \times T_{10} + A_{32} \times T_{10}^2 \end{cases} \end{cases}, \quad (2)$$

where B is the instantaneous bias (°C/h), B_0 is the average bias in the former two minutes (°C/h), T_1 is the temperature of position P1 (°C), T_{10} is the first temperature of position P1 (°C), T_2 is the temperature of position P2 (°), a_1, a_2, a_3 and A_{1j}, A_{2j}, A_{3j} $(j = 0, 1, 2)$ are the model fit coefficients.

In the model, as Eq. (2), the first item delegates the main part of the bias, and the second delegates the influence on the bias owing to the variance of temperature, and the third is the quadratic of the variance of temperature, and the fourth shows the influence due to the velocity of temperature. The latter three items show that the change and fluctuation surround the main part of the bias. Compared with other models, the model has obvious advantages. It adopts the average bias in the former two minutes after RLG is working as the main part of the bias, and the variety, grads and quadratic of the temperature are considered as the model parameters. Owing to these small variables, in the real-time compensating, it will not lead to large estimate error even when the calculated number of the coefficient has a little error compared with the ideal number, therefore, the whole compensating effect is good.

When the temperature measured from different temperature sensing points is adopted as its independent variable to fit the bias curve in the model, obviously the accuracy is different. Here we adopt the sum of squares

of the error ($\mathrm{SSE_{ave}}$) to show the model fit accuracy

$$\mathrm{SSE_{ave}} = \frac{1}{m}\sum_{j=1}^{m}\sum_{i=1}^{n}(y_i - \hat{y}_i)^2, \tag{3}$$

where y_i is the practical output of RLG, $\hat{y}_i$ is the estimate output value according to the temperature compensating model, n is the data number in a test temperature point, m is the number of test temperature point. From Eq. (3), we can see that the smaller the $\mathrm{SSE_{ave}}$ is, the higher the compensating model fit accuracy is.

The typical six combinations of the temperature sensing point such as (P1 and P2), (P1 and P4), (P2 and P4), (P3 and P2), (P3 and P4), (P4 and P3) are marked as M1, M2, M3 ,M4, M5, and M6 left each other. When we adopt the above six combinations to build the compensating model, and use them to compensate the test data of RLG in the different given surrounding temperatures, the $\mathrm{SSE_{ave}}$ value will be different, and the $\mathrm{SSE_{ave}}$ value of six compensating models with a group teat data is shown in Table 1.

From Table 1, we can see that the model M1 has the best compensating effect, so the angular rate sensor and the anode are the best temperature sensing points of the RLG.

In the engineering, we can test every RLG in detail, and according the test data and the compensating model we can get their fit coefficients a_1, a_2, a_3 and A_{1j}, A_{2j}, A_{3j} $(j = 0, 1, 2)$, then we can solidify the fit coefficients into the computer. In the use of RLG, We sample the first temperature T_{10} and the average bias of the former two minutes when RLG is working, then we minutely sample the temperatures T_1 and T_2, and in this way we can estimate the current bias and then have a real-time compensating.

First, we newly have two kinds of experiments in the given surrounding temperature and in the mutative temperature from 20 to 60 °C respectively. Then we adopt the compensating model to have a real-time compensating. The bias and fit curve under part given surrounding temperature are shown in Fig. 5. The compensating results under given surrounding temperatures are shown in Fig. 6 and Table 2.

From above, the result under the given surrounding temperature is well. Especially under 60 °C, because its

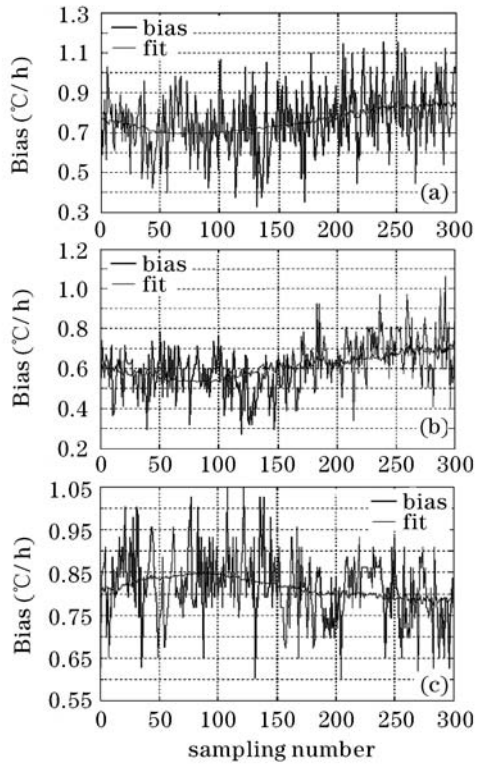

Fig. 5. Bias and fit curves under the given surrounding temperature (part). (a) Bias and fit curves under 40 °C; (b) bias and fit curves under 0 °C; (c) bias and fit curves under −20 °C.

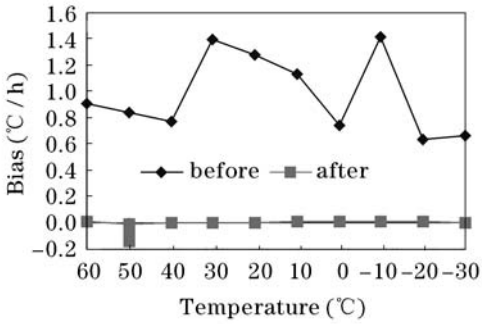

Fig. 6. Compensating results in the given surrounding temperature.

Table 1. $\mathrm{SSE_{ave}}$ Value of Six Compensating Models

T (°C)	$\mathrm{SSE_{ave}}$ (°C/h)					
	M1	M2	M3	M4	M5	M6
50	1.0682	1.0781	1.0807	1.0792	1.1224	1.2058
40	1.3878	1.4145	1.4294	1.4306	1.4965	1.5012
30	1.5368	1.5864	1.5378	1.5243	1.5368	1.5624
20	1.9875	2.0134	2.0456	2.037	2.0368	2.1435
10	1.2356	1.2987	1.3698	1.4215	1.3697	1.5687
0	1.5684	1.6847	1.6974	1.7685	1.8126	1.8456
−10	3.1264	3.2654	3.6544	3.9875	3.6845	3.6981
−20	4.5232	4.5448	4.8369	4.8092	4.8321	4.9635
−30	2.0299	2.0401	2.0585	2.0448	2.1245	2.0574
$\mathrm{SSE_{ave}}$	2.0515	2.1029	2.1900	2.2336	2.2239	2.2829

Table 2. Bias and Bias Stability of Compensating Result in the Given Surrounding Temperature

T (°C)	Bias (°C/h)		Bias Stability (°C/h)	
	Before	After	Before	After
60	0.9035	0.0098	0.0562	0.0521
50	0.8334	−0.0093	0.0334	0.0289
40	0.7667	−0.0082	0.0492	0.0414
30	1.3985	−0.0091	0.0460	0.0414
20	1.2764	−0.0087	0.1075	0.0515
10	1.1341	0.0064	0.0675	0.0580
0	0.7368	0.0068	0.0776	0.0628
−10	1.4169	0.0093	0.2042	0.0710
−20	0.6307	0.0082	0.0910	0.0521
−30	0.6573	−0.0079	0.0589	0.0589

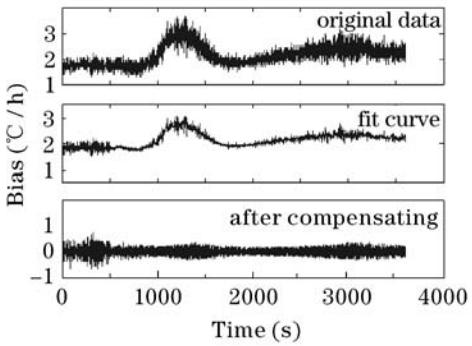

Fig. 7. Compensating results in the mutative temperature.

data is not used to fit the model, but the compensating result is relatively good.

In addition, a test data under the mutative surrounding temperature from 20 to 50 °C are also used to fit and compensate, as shown in Fig. 7, the compensating effect is also good.

In conclusion, the compensating technique especially adapts to those changes with temperature, for example, fall first and rise then, rise first and fall then. The bias after compensating is reduced to below 0.01 °C/h, and the change trend of the bias changing with the temperature is eliminated. That is to say, whatever surrounding temperature is, when the input is zero angular-rate, the output of RLG is zero by and large, and at the same time, the bias stability is enhanced too. The most important is that the model can quite meets the requirement of real-time compensation and it is valuable to the practical application of RLG.

This work was partially supported by the Doctorate Foundation of Engineering College, the Air Force Engineering University. C. Cuo's e-mail address is guochuangdoc@163.com or 737086@sina.com.

References

1. Y. Jiang, *Ring Laser Gyro* (Publishing Company of Tsinghua, Beijing, 1985).
2. G. Xu, *RLG Predominate the Market of the Present-Day Gyroscope* (Development and Research Center of the Aviation Industry of China, Xi'an 2005).
3. G. Wu, Q. Gu, and X. Zheng, J. Tsinghua Univ. (Sci. & Tech.) **43,** 180 (2003).
4. F. Qian, W. Tian, Y. Yang, and Z. Jin, J. Optoelectron.·Laser (in Chinese) **14,** 124 (2003).
5. J. Wang, C. Guo, R. Fan, and X. Zhao, in *Proceedings of ICEMI'2005* pp.724—727 (2005).
6. X. Zhao, X. Li, and B. Lei, Chin. Inertia Technique Transaction (in Chinese) **12,** 55 (2004).
7. H. Zhou, J. Liu, Z. Xiong, and J. Lai, Opto-Eletron. Eng. (in Chinese) **33,** 135 (2006).